Journal of Quantitative Spectroscopy & Radiative Transfer 178 (2016) 224–229

Contents lists available at ScienceDirect

Journal of Quantitative Spectroscopy & Radiative Transfer

journal homepage: www.elsevier.com/locate/jqsrt

Optical resonances in electrically charged particles and their relation to the Drude model

Miroslav Kocifaj [a,b,*], František Kundracik [b], Gorden Videen [c], Alex J. Yuffa [c], Jozef Klačka [b]

[a] ICA, Slovak Academy of Sciences, Dúbravská Road 9, 845 03 Bratislava, Slovak Republic
[b] Department of Experimental Physics, Faculty of Mathematics, Physics, and Informatics, Comenius University, Mlynská dolina, 842 48 Bratislava, Slovak Republic
[c] Army Research Laboratory, Adelphi, MD 20783, United States

ARTICLE INFO

Article history:
Received 14 September 2015
Received in revised form
22 October 2015
Accepted 25 November 2015
Available online 2 December 2015

Keywords:
Electromagnetic scattering
Charged particles
Drude model

ABSTRACT

The Drude model is conventionally used to explain the average motion of electrons in typical material. In this paper, we analyze the individual terms of the Drude model in order to uncover their influence on the scattering properties of small particles. Namely, a query on whether resonance enhancement is due to optical effects or the conductivity model. This query arose from our earlier theoretical and numerical experiments and still remains unresolved today. We show that certain resonance features are caused primarily by the interaction of the electromagnetic wave with the excess electric charge on the particles. Furthermore, we show that the role of a conductivity model is limited to only establishing the relative importance of the inertial moment of the carriers and the viscous drag forces. For frequencies $\omega \leq k_B T/\hbar$, the viscous forces only cause minor damping effects and the change in the peak resonance (along with its amplitude) are caused by the electric and inertial forces. These forces dominate because the viscous forces quickly decay with decreasing temperature.

In order to demonstrate the optical behavior of charged water droplets, we construct a Mie-series solution with modified boundary conditions that properly account for the excess electric charge on the droplets. Our solution explains the weak scattering enhancement for frequencies far beyond the resonance, and it also predicts an absorption resonance edge in the long-wavelength limit.

Our findings are not only useful to theoreticians who focus on the individual parameters such as the viscous term in the Drude model and/or search for better surface conductivity models, but also to experimentalists who gather as much data as possible in order to ascertain how the numerically determined optical properties compare with the experimental measurements.

1. Introduction

An excitation of localized surface plasmons is well-known in metalic nanosized particles [17,6]. The surface modes in small spherical particles occur when the denominators of the Mie scattering coefficients vanish or approach zero [2]. However, it only recently has been proven that the small electrically charged particles can also resonate in a number of modes with the incident electromagnetic wave [16,21]. These surface excitations are closely related to the surface charge density [3] that is composed of static and oscillatory components [13]. Moreover, the excitations are also related to the

* Corresponding author.
E-mail address: kocifaj@savba.sk (M. Kocifaj).

http://dx.doi.org/10.1016/j.jqsrt.2015.11.021
0022-4073/

flow of charges because they can change the tangential electric field on the surface of the particle. Both of these quantities are related to the surface conductivity and to the following processes: (i) the movement of the unbounded charge on the surface of the particle, (ii) the passing of the surplus electrons into an empty conduction band and/or (iii) the polarization of the surplus electrons in a surface-bound state [10,18]. The classical phenomenological model developed by Paul Drude, namely, the Drude model, [5] was not intended to describe the conductivity enhancement caused by the above processes. However, the Drude approach is still preferred because it accounts for both the inertial and the viscous drag forces experienced by the transport electrons.

Although the Drude model is quite general, the above-mentioned forces only roughly approximate the actual interactions between the electrons and the ions. For instance, the damping coefficient used in the viscous drag force formula is modeled to be proportional to $k_B T/\hbar$ in many materials (here k_B is the Boltzmann constant, T is the temperature of the particle, and $\hbar$ is the reduced Planck constant). However, the proportionality constant is only a rough estimate and not exact. Previously, we have demonstrated that the far-field as well as the near-field optical signatures of the electrically charged particles differ from the signatures of neutral particles. Furthermore, we have shown that the parameters such as the surface conductivity or $k_B T/\hbar$ work as modulators of the optical response (see e.g. [18,14,11]; and also [4,22]). It is only in the last few years that the effects on the scattering properties caused by the excess electric charge, the surface potential, or the temperature were recognized. In electrified particulate systems, the above-mentioned causes are among the largest sources of uncertainty in predictions of collective optical effects. Undoubtedly, the role of the Drude model in the optical resonances has to be uncovered before any reasonable conclusions can be made regarding the features contained in the optical signature of the charged particles. In this case, the wavelength λ should be varied instead of the particle radius a because the effects of the Drude model will stay hidden when the optical characteristics are computed as a function of the size parameter $x=2\pi a/\lambda$. In other words, the frequency-dependent conductivity is required to demonstrate how the Drude model influences the optical response of the small particles.

2. Theoretical formulation of scattering by charged particles

In the Drude model the time constant τ, which characterizes the average time between collisions, is used to approximate the interaction between the charge carriers. In this concept, the probability of collision (attenuation rate) is proportional to $1/\tau$. The classical approach to model the 3D volume charges dictates that a free charge carrier of mass M and electric charge q is decelerated by a fictitious (phenomenological) friction force [12,19]. The motion of the charge carriers is described by

$$\dot{\mathbf{u}} = \frac{q}{M}\mathbf{E} - \frac{1}{\tau}\mathbf{u}, \tag{1}$$

where u is the velocity, and **E** is the electric field vector. If the charge is deposited on the surface of a sphere, then Eq. (1) becomes

$$\dot{\mathbf{u}}_t = \frac{q}{M}\mathbf{E}_t - \gamma_s \mathbf{u}_t, \tag{2}$$

where $\mathbf{u}_t$ denotes the velocity component that is tangential to the surface of the sphere, and γ_s is the mass-normalized damping coefficient. The damping coefficient γ_s can be expressed as an inverse of the relaxation time and is proportional to $k_B T/\hbar$ in many materials (e.g. metal). In this work, we assume the proportionality factor is unity and thus we have $\gamma_S = k_B T/\hbar$.

It is easy to show [11] that $\sigma_s = i\rho_{S0} e/\left[(\omega + i\gamma_S) M_e\right]$ in a case of a harmonic incident wave, where $M_e = 9.109 \times 10^{-31}$ kg, $e = 1.602 \times 10^{-19}$ C, i is the imaginary unit, ω is the angular frequency, and ρ_{S0} is the static component of the surface charge density. After a bit of manipulation, we can express the surface conductivity as a non-linear function of γ_s, namely,

$$\sigma_S = \frac{gk}{i\omega\mu_0} = \frac{k}{\omega\mu_0}\frac{x}{2}\frac{\omega_S^2}{\omega^2+\gamma_S^2}\left(\frac{\gamma_S}{\omega} + i\right), \tag{3}$$

where k is the wavenumber, ω_S is the surface plasma frequency (see [3])

$$\omega_S^2 = 2\frac{e}{M_e}\frac{\Phi}{a^2}, \tag{4}$$

and Φ is the electrostatic potential on the surface of the uniformly charged sphere of radius a.

Note that for low frequencies ($\omega << \gamma_S$) the electric conductivity is a purely real quantity that is inversely proportional to γ_s. In contrast, at high frequencies the conductivity is purely imaginary quantity that is proportional to the ratio e/M_e and is independent of the damping coefficient γ_s.

The optical response of a charged particle can be obtained from Maxwell equations subject to appropriate boundary conditions and certain constitutive relations [20]. However, the boundary conditions for an electrically charged particle and for an electrically neutral particle are different. In order to derive these boundary conditions, we will deal with the integral form of the Maxwell equations as well as the continuity equation.

Let us consider a small cuboid of volume $V = S_\perp\, \Delta h$ and with the surfaces $S_\perp = X\,Y$, $X\,\Delta h$, and $Y\,\Delta h$. The bottom base of the cuboid is situated in medium 1 and the top surface is in medium 2 (Fig. 1). If the surface area $S_\perp$ has free electric charges with the surface charge density ρ_S, then the total electric charge of the small cuboid is

$$Q = \int_V \rho dV = \int_{S_\perp} \rho_S dS_\perp. \tag{5}$$

The rate of change of this charge is

$$-\frac{dQ}{dt} = \oint_S \mathbf{j}\cdot d\mathbf{S} = \int_{S_\perp} \mathbf{j}\cdot d\mathbf{S}_\perp + \oint_{l_\perp} \mathbf{j}_S \cdot d\mathbf{l}_\perp, \tag{6}$$

where $\mathbf{j}_S$ is the surface current density, $d\mathbf{S}_\perp$ is an elementary

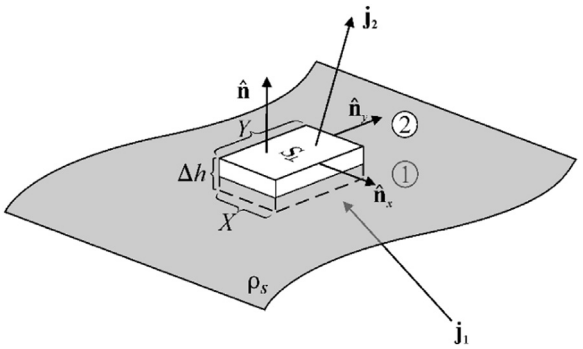

Fig. 1. Schematic representation of boundary conditions.

surface perpendicular to the surface $S_\perp$, ($d\mathbf{S}_\perp = \hat{\mathbf{n}} dS_\perp$), S is the total surface of the cuboid depicted in Fig. 1, and $l_\perp$ is the circumference of the area $S_\perp$. The above equations can be written as

$$-\frac{dQ}{dt} = -\frac{\partial \rho_S}{\partial t} S_\perp$$

and

$$\oint_S \mathbf{j} \cdot d\mathbf{S} = \hat{\mathbf{n}} \cdot (\mathbf{j}_2 - \mathbf{j}_1) S_\perp + (\nabla \cdot \mathbf{j}_S) S_\perp, \tag{7}$$

respectively, where $\mathbf{j}_1$ and $\mathbf{j}_2$ are the volume current densities (measured in $\mathrm{A\,m^{-2}}$), and $\mathbf{j}_S$ is the surface current density (measured in $[\mathrm{A\,m^{-1}}]$). The second term on the right-hand side of Eqs. (6) and (7) is identical. To see this, we write the second term on the right-hand side of Eq. (6) as

$$\oint_{l_\perp} \mathbf{j}_S \cdot d\mathbf{l}_\perp = \mathbf{j}_S(x,y) \cdot (-\hat{\mathbf{n}}_x) Y + \mathbf{j}_S(x+X,y) \cdot (\hat{\mathbf{n}}_x) Y + \mathbf{j}_S(x,y) \cdot (-\hat{\mathbf{n}}_y) X + \mathbf{j}_S(x,y+Y) \cdot (\hat{\mathbf{n}}_y) X, \tag{8}$$

where X and Y are the lengths of the small rectangular surface $S_\perp$ when measured along the x- and y-axes, respectively. Using Taylor series expansion, we obtain

$$\oint_{l_\perp} \mathbf{j}_S \cdot d\mathbf{l}_\perp = \left(\frac{\partial \mathbf{j}_S}{\partial x} \cdot \hat{\mathbf{n}}_x\right) XY + \left(\frac{\partial \mathbf{j}_S}{\partial y} \cdot \hat{\mathbf{n}}_y\right) XY = (\nabla \cdot \mathbf{j}_S) S_\perp. \tag{9}$$

Thus, from Eq. (9) we conclude that the two terms are indeed identical. Moreover, by using Eq. (9), it is easy to show that the boundary condition for the current density is

$$\nabla_S \cdot \mathbf{j} \equiv \hat{\mathbf{n}} \cdot (\mathbf{j}_2 - \mathbf{j}_1) = -\frac{\partial \rho_S}{\partial t} - (\nabla \cdot \mathbf{j}_S). \tag{10}$$

where the symbol *Div* denotes the surface divergence. For an alternative derivation of Eq. (10) please see [1].

To derive the boundary conditions satisfied by the H-field, let us consider a closed curve in the form of a narrow rectangle as shown in Fig. 2. Applying the Stokes theorem to the first Maxwell equation (Ampere's law), we obtain

$$\int_{S_\parallel} (\nabla \times \mathbf{H}) \cdot d\mathbf{S}_\parallel = \oint_C \mathbf{H} \cdot d\mathbf{r} = \int_{S_\parallel} \mathbf{j} \cdot d\mathbf{S}_\parallel + \int_{S_\parallel} \frac{\partial \mathbf{D}}{\partial t} \cdot d\mathbf{S}_\parallel. \tag{11}$$

In Eq. (11), $d\mathbf{S}_\parallel$ is an elementary surface oriented perpendicularly to the surface $S_\parallel = X\,\Delta h$ (i.e. $d\mathbf{S}_\parallel$ has the orientation of the local normal $\hat{\mathbf{n}}'$). From the geometry of the problem we also have that

$$\oint_C \mathbf{H} \cdot d\mathbf{r} = (\mathbf{H}_2 - \mathbf{H}_1) \cdot (\hat{\mathbf{n}}' \times \hat{\mathbf{n}}) X, \tag{12}$$

where the unit vector $\hat{\mathbf{n}}$ is normal to the local surface, and $\hat{\mathbf{n}} \cdot \hat{\mathbf{n}}' = 0$.

Over an infinitesimally small rectangle with the area $S_{\parallel = X\,\Delta h}$, the integral $\int_{S_\parallel} \frac{\partial \mathbf{D}}{\partial t} \cdot d\mathbf{S}_\parallel$ approaches zero when the width of the rectangle Δh vanishes. Nevertheless, the right-hand-side of the integral $\int_{S_\parallel} \mathbf{j} \cdot d\mathbf{S}_\parallel$ is equal to

$$\int_{S_\parallel} \mathbf{j} \cdot d\mathbf{S}_\parallel = \mathbf{j} \cdot \hat{\mathbf{n}}' S_\parallel = \mathbf{j} \cdot \hat{\mathbf{n}}' X \Delta h = \mathbf{j}_S \cdot \hat{\mathbf{n}}' X, \tag{13}$$

where $\mathbf{j}_S = \mathbf{j} \Delta h$ is the surface current density. By comparing Eqs. (12) and (13) we obtain

$$(\mathbf{H}_2 - \mathbf{H}_1) \cdot (\hat{\mathbf{n}}' \times \hat{\mathbf{n}}) = \mathbf{j}_S \cdot \hat{\mathbf{n}}', \tag{14}$$

and a bit of manipulation yields the desired result, namely,

$$\hat{\mathbf{n}} \times (\mathbf{H}_2 - \mathbf{H}_1) = \mathbf{j}_S. \tag{15}$$

For an alternative and more lavish derivation of Eq. (15) see [1]. In contrast to Eq. (15), the corresponding equation for an electrically neutral particle is

$$\hat{\mathbf{n}} \times (\mathbf{H}_2 - \mathbf{H}_1) = 0. \tag{16}$$

The surface current density $\mathbf{j}_S$ is non-zero if $\partial \rho_S / \partial t \neq 0$ (also see Eq. (10)). Applying the Stokes theorem to the third Maxwell equation (Faraday's law) we immediately find that

$$\int_{S_\parallel} (\nabla \times \mathbf{E}) \cdot d\mathbf{S}_\parallel = \oint_C \mathbf{E} \cdot d\mathbf{r} = \int_{S_\parallel} -\frac{\partial \mathbf{B}}{\partial t} \cdot d\mathbf{S}_\parallel, \tag{17}$$

where the right-hand side equals zero when the width of the rectangle (Δh) vanishes. Therefore, Eq. (17) transforms into a simple form, namely,

$$(\mathbf{E}_2 - \mathbf{E}_1) \cdot (\hat{\mathbf{n}}' \times \hat{\mathbf{n}}) = 0, \tag{18}$$

and similarly we find that

$$\hat{\mathbf{n}} \times (\mathbf{E}_2 - \mathbf{E}_1) = 0. \tag{19}$$

We use the above derived boundary conditions and the separation-of-variables method to obtain the modified formulae for Mie expansion coefficients [11] of a charged sphere of radius a; namely,

$$a_n = \frac{\mu_2^{-1} \psi_n(x) \psi_n'(m\,x) - m \mu_1^{-1} \psi_n'(x) \psi_n(m\,x) - i\,\omega\,k^{-1} \sigma_s \psi_n'(x) \psi_n'(m\,x)}{\mu_2^{-1} \xi_n(x) \psi_n'(m\,x) - m \mu_1^{-1} \xi_n'(x) \psi_n(m\,x) - i\,\omega\,k^{-1} \sigma_s \xi_n'(x) \psi_n'(m\,x)} \tag{20}$$

and

$$b_n = \frac{\mu_2^{-1} \psi_n'(x) \psi_n(m\,x) - m \mu_1^{-1} \psi_n(x) \psi_n'(m\,x) + i\,\omega\,k^{-1} \sigma_s \psi_n(x) \psi_n(m\,x)}{\mu_2^{-1} \xi_n'(x) \psi_n(m\,x) - m \mu_1^{-1} \xi_n(x) \psi_n'(m\,x) + i\,\omega\,k^{-1} \sigma_s \xi_n(x) \psi_n(m\,x)}, \tag{21}$$

where μ_1 and μ_2 are the permeability of the scatterer and the permeability of the surrounding media, respectively, and $x = 2\pi a/\lambda$ is the size parameter. In Eqs. (20) and (21), λ is the wavelength of the incident radiation, the prime denotes differentiation with respect to the argument, and $\psi_n(x)$ and $\xi_n(x)$ are defined in terms of Bessel and Hankel functions. In contrast to the electrically neutral sphere,

Eqs. (20) and (21) contain additional terms that are proportional to the surface conductivity σ_s.

In the following sections, we will analyze the optical properties of the electrically charged sphere for a wide range of size parameters by using the frequency-dependent surface conductivity formula (3) and Mie expansion coefficients (Eqs. (20) and (21)) that were derived from the boundary conditions given by Eqs. (10) and (15).

3. Toward the Drude model constituents, surface conductivity and extinction efficiency

The frequency-dependent conductivity given by Eq. (20) depends on two parameters, namely, the surface potential Φ and the mass-normalized damping coefficient γ_s. For a fixed particle size, the surface potential is directly proportional to the plasma frequency ω_S^2 and thus, the plasma frequency is determined by the potential. In other words, the surface potential is a key factor influencing the optical effects; however, it does not determine how σ_s depends on frequency. In contrast, the surface conductivity is a non-trivial function in both γ_s and ω. Obviously, the optical properties of charged particles change with γ_s because γ_s characterizes the fictitious viscous forces experienced by the electrons. For example, small γ_s implies a long coherence time, which means that the viscous forces are relatively weak.

We demonstrate these effects numerically by computing the extinction cross-section Q_{ext} via the method outlined in Section 2. For this purpose, we simulate light scattering from a spherical particle of radius 0.01 μm and charged to a potential of 5 V (for these parameters, the plasma frequency is 2.1×10^{13} Hz). We vary the incident wavelength from 0.6 to 500 μm, i.e. the corresponding size parameter varies from 0.0001 to 0.1. The ratio of the efficiency factors for the charged and an identical uncharged sphere is shown in Fig. 3 as a function of the size parameter. To help with the interpretation of Fig. 3, we show $\sigma_s(x)$ in Fig. 4 for $\Phi=5$ V and $T=100$ K.

From Fig. 3, we see that the net surface charge causes the amplification rate to reach its maximum at roughly $x_P\approx 2\times10^{-3}$. Furthermore, from Fig. 4 we also see that the imaginary part of the surface conductivity is larger than the real part if x is near the resonance peak. For these size parameters, the acceleration of the surface electrons is mainly due to the electric force and the inertial mass of electrons while the effects caused by the viscous drag forces are negligible. The amplitude of the viscous forces

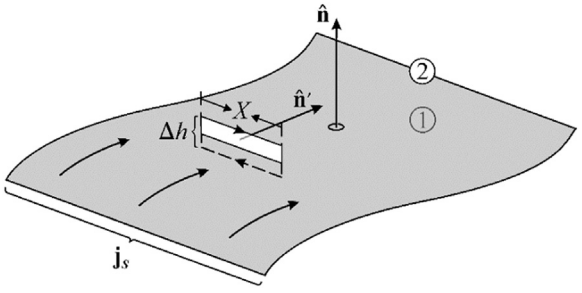

Fig. 2. The evaluation of the boundary conditions for the H-field.

quickly decays with decreasing temperature, especially when the temperature is near zero. On the other hand, high temperatures imply enhanced viscous forces; therefore, the temperature is an important modulator of the extinction efficiency factor for the size parameters $x<x_P$, while the effect of the temperature on Q_{ext} disappears for $x>\approx 10x_P$. In general, γ_s works as a damping coefficient that efficiently suppresses and smooths the resonant peak in Q_{ext} (see Fig. 3). In fact, ω and γ_s enter Eq. (20) in a ratio, thus, ω can be thought of as a "strength" measure of γ_s. Thus we conclude that the viscous forces only play a decisive role when $\omega\le\gamma_s$, i.e. $\omega\le k_BT/\hbar$.

4. Explanation and prediction of some anomalous experimental results

Experiments on the optical behavior of isolated electrically charged particles (that is a problem different from what we know as surface plasmon polaritons) are still rare. For example, amplified microwave attenuation in sandstorms [8] remained unexplained until it was shown that the Rayleigh theory is an insufficient formulation to describe electromagnetic scattering by small charged particles [13,15]. These researchers demonstrated that there are some physical quantities that cannot be predicted accurately by the conventional models because these models do not account for the excess charge. Thus, the formulation presented in this paper, which uses the modified boundary conditions, can potentially be used to explain a number of anomalous experimental results that have challenged the electromagnetic community. In the next paragraph, we will describe one such challenge in some detail.

Heifetz et al. [9] performed laboratory measurements on charged water droplets, which were theoretically modeled by dielectric spheres with diffusion-deposited mobile surface charges. In this experiment, the potential difference appears in a double-layer structure on the surface of a scattering particle; however, we are using a model of a negatively charged particle with electrons on the surface of the droplet. We note that our approach is similar to the one used by Geldart and Chýlek [7]. Although Heifetz et al. confirmed the optical properties of the water droplet's response to a time-dependent air-ionization profile, the changes in the optical characteristics such as backscatter amplitude were too low. In fact, they were as low as 1% at 94 GHz. We have theoretically reproduced the above-mentioned experimental results and also found very low amplitudes for the scattering efficiency in the 90–95 GHz frequency interval, see Fig. 5.

Using our formulation, which depends on a phenomenological surface conductivity but is theoretically sound, we found that the optical effects are marginal at the above mentioned frequencies. Specifically, the operating frequency of 94 GHz is beyond the resonance region as evident from Figs. 5 and 6, which show normalized scattering efficiencies as a function of wavelength. The theoretical value of the amplification factor for charged particles $Q_{sca}(c)$ is only a few percent higher than that for electrically neutral water droplets even if the surface potential is close to Rayleigh limit (see

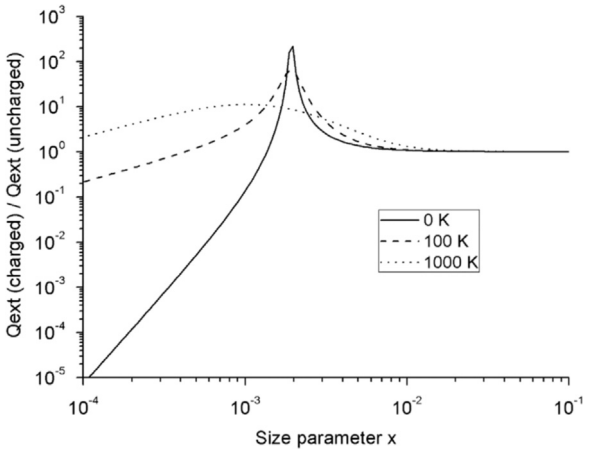

Fig. 3. The ratio of the extinction efficiency factors for the charged and an identical uncharged particle is shown as a function of the size parameter x for temperatures 0 K, 100 K, and 1000 K.

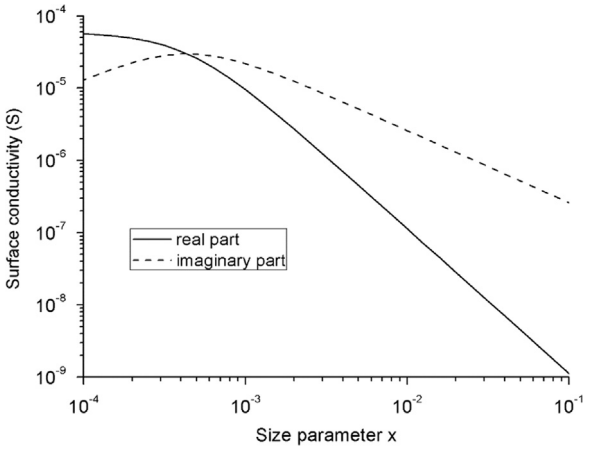

Fig. 4. The surface conductivity σ_s (with $T=100$ K) is shown as a function of the size parameter x.

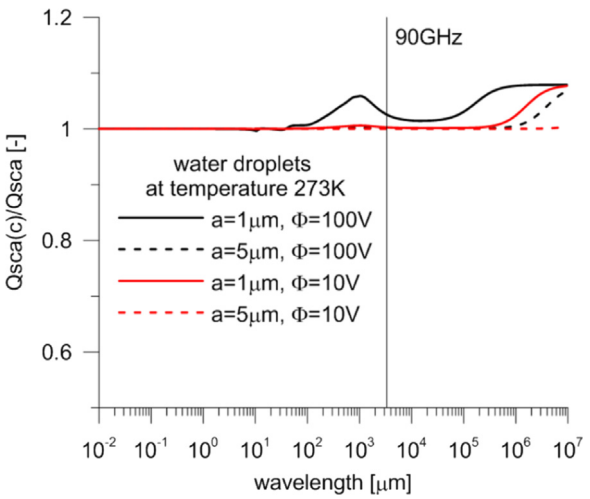

Fig. 5. Theoretical efficiency factor as a ratio of scattering cross-sections for the charged and an identical uncharged water droplets is shown as a function of the wavelength.

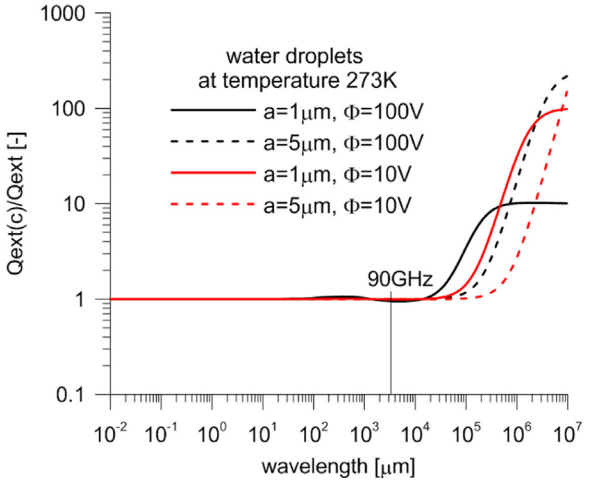

Fig. 6. The same as in Fig. 5 but for the extinction cross-section. Notice that the absorption effects dominate near the resonance edge.

Fig. 5: for a particle radius of 1 μm and surface potential 100 V, the Rayleigh limit is about 180 V). The far-field optical resonances are generally low for scattered radiation, but might be large if absorption is present, as was demonstrated by Kocifaj et al. [15]. To reach the resonance behavior it would be necessary to either decrease the operating frequency (by increasing the wavelength), or greatly reduce the particle size. However, from Figs. 5 and 6 we see that the main resonance arises due to absorption and not due to scattering—notice that the curves shown in Fig. 6 account for both scattering and absorption, while curves in Fig. 5 only account for scattering.

5. Conclusions

We have analyzed how the parameters of the Drude model can determine the optical properties of charged particles, and whether the Drude model causes the resonance edge in plasmon-related absorption. We found that the Drude model appears to be applicable in modeling the surface conductivity σ_S. Moreover, we demonstrated that the imaginary component of the surface conductivity significantly influences the scattering properties of small particles, while its real component only has a damping effect at low frequencies. The surface potential Φ works exclusively as a scale factor, i.e., a constant of proportionality in the expression for σ_S. Essentially, Φ only determines the strength of the effects studied in this paper. Thus, the absorption (and/or scattering) enhancement at certain wavelengths is caused by optical resonances and not dictated by a chosen conductivity model because the conductivity model shows no extrema at these wavelengths.

The maximum amplification of Q_{ext} occurs near zero temperature because the viscous forces are weak and both the electric and inertial forces dominate. This finding alone can explain why the optical effects caused by the net surface charges are also important for insulators such as SiO_2 [18]. To see this, we first note that even in bound surface states, the excess electrons can polarize due to the electric field. Therefore, the inertial and elastic forces are the decisive ingredients,

while the viscous forces have only minor, typically damping, effects.

For small size parameters and frequencies $\omega \leq k_B T/\hbar$, the viscous term is responsible for lowering Q_{ext} and, generally speaking, is small near the peak resonance for temperatures 10–100 K. In order to better understand the optical phenomena due to the excess charges, we show that it is necessary to consider viscous forces and their effects on the motion of the electrons confined to the surface of the particle.

We successfully apply the surface conductivity model to predict and explain the experimental results dealing with the scattering properties of electrically charged water droplets. These properties deviate only marginally from those of uncharged particles because the operating frequency used in the experiment was far beyond the resonance regime. Furthermore, we demonstrate that the resonant amplification can be reached by modifying the incident frequency.

There is no doubt that knowledge of the optical properties of electrically charged particles can be applied in diverse fields of science, especially in atmospheric science. For example, characterizing water droplets in ocean sprays, ice crystals in thunderstorms, atmospheric aerosols, aerosolized agents, pollution, or dust. To understand the electromagnetic interaction with these particles, a targeted theoretical model must be developed and complemented by actual experiments, where the incident wavelength, particle size, permittivity, permeability, surface charges, and temperature can be varied. In fact, the role of temperature in electromagnetic scattering by a charged particle is still not completely clear. Therefore, further theoretical, numerical, and experimental studies are required to provide satisfactory answers to fundamental scattering questions dealing with optical signatures of charged particles.

Acknowledgments

This work was supported by the US Army International Technology Center under the contract no.: W911NF-14-1-0601 (R&D 1695-PH-01) and by the US Army Research Laboratory under the contract no.: W911NF-12-2-0019. The computational work was supported by the Slovak National Grant Agency VEGA (Grant no. 2/0002/12).

References

[1] Arnoldus HF. Conservation of charge at an interface. Opt Commun 2006;265:52–9.
[2] Bohren C, Huffman D. Absorption and scattering of light by small particles. New York: John Wiley & Sons; 1983.
[3] Bohren CF, Hunt AJ. Scattering of electromagnetic waves by a charged sphere. Can J Phys 1977;55:1930–5.
[4] Chung HY, Leung PT, Tsai DO. Effects of extraneous surface charges on the enhanced Raman scattering from metallic particles. J Chem Phys 2013;138:224101.
[5] Dressel M, Gräuner G. Electrodynamics of solids: optical properties of electrons in matter. Cambridge, UK: Cambridge University Press; 2002.
[6] Fan X. Light scattering and surface plasmons on small spherical particles. Light: Sci Appl 2014;3:e179.
[7] Geldart DJW, Chýlek P. Absorption of solar radiation by charged water droplets. J Quant Spectrosc Radiat Transf 2001;70:697–708.
[8] Haddad S, Salman MJH, Jha RK. Effect of dust/sand storms on some aspects of microwave propagation. In: Proceedings of the Ursi Commission F Symposium (ESA, 1983); 1983. p. 153–161.
[9] Heifetz A, Chien HT, Liao S, Gopalsami NS, Raptis ACP. Millimeter-wave scattering from neutral and charged water droplets. J Quant Spectrosc Radiat Transf 2010;111:2550–7.
[10] Heinisch RL, Bronold FX, Fehske H. Optical signatures of the charge of a dielectric particle in a plasma. Phys Rev E 2013;88:023109.
[11] Klačka J, Kocifaj M. Scattering of electromagnetic waves by charged spheres and some physical consequences. J Quant Spectrosc Radiat Transf 2007;106:170–83.
[12] Klačka J, Kocifaj M. On the scattering of electromagnetic waves by a charged sphere. Prog Electromagn Res 2010;109:17–35.
[13] Klačka J, Kocifaj M, Kundracik F, Videen G. Optical signatures of electrically charged particles: fundamental problems and solutions. J Quant Spectrosc Radiat Transf 2015;164:45–53.
[14] Kocifaj M, Klačka J. Scattering of electromagnetic waves by charged spheres: near-field external intensity distribution. Opt Lett 2012;37:265–7.
[15] Kocifaj M, Klačka J, Kundracik F, Videen G. Charge-induced electromagnetic resonances in nanoparticles. Ann der Phys 2015;527(11–12):765–9. http://dx.doi.org/10.1002/andp.201500202.
[16] Kocifaj M, Klačka J, Videen G, Kohút I. Optical properties of a polydispersion of small charged cosmic dust particles. J Quant Spectrosc Radiat Transf 2012;113:2561–6.
[17] Kottmann JP, Martin S. Spectral response of plasmon resonant nanoparticles with a non-regular shape. Opt Express 2000;6:213–9.
[18] Kundracik F, Kocifaj M, Videen G, Klačka J. Effect of charged-particle surface excitations on near-field optics. Appl Opt 2015;54:6674–81.
[19] Meschede D. Optics, light and lasers. 2nd editionWeinheim: Wiley-VCH Verlag; 88.
[20] Mishchenko MI. Electromagnetic scattering by particles and particle groups: an introduction.Cambridge: Cambridge University Press; 2014.
[21] Rosenkrantz E, Arnon S. Enhanced absorption of light by charged nanoparticles. Opt Lett 2010;35:1178–80.
[22] Wang N, Liu S, Lin Z. Tailoring optical properties of surface charged dielectric nanoparticles based on an effective medium theory. Opt Express 2013;21(17):20387–93.